Journal of Molecular Catalysis A: Chemical 313 (2009) 14–21

Contents lists available at ScienceDirect

Journal of Molecular Catalysis A: Chemical

journal homepage: www.elsevier.com/locate/molcata

Selective alcohol oxidation to aldehydes and ketones over base-promoted gold–palladium clusters as recyclable quasihomogeneous and heterogeneous metal catalysts

P.G.N. Mertens[a], S.L.F. Corthals[a], X. Ye[b], H. Poelman[c], P.A. Jacobs[a], B.F. Sels[a], I.F.J. Vankelecom[a], D.E. De Vos[a,*]

[a] Centre for Surface Chemistry and Catalysis, K.U.Leuven, Kasteelpark Arenberg 23, 3001 Leuven, Belgium
[b] Department of Metallurgy and Materials Engineering, K.U.Leuven,, Kasteelpark Arenberg 44, 3001 Leuven, Belgium
[c] Department of Solid State Science, U.Gent, Krijgslaan 281 S1, 9000 Gent, Belgium

ARTICLE INFO

Article history:
Received 27 January 2009
Received in revised form 12 July 2009
Accepted 16 July 2009
Available online 24 July 2009

Keywords:
Alcohol oxidation
Solvent-free oxidation
Quasihomogeneous catalyst
Heterogeneous catalyst
Bimetallic catalyst
Gold
Palladium
Spinel
Solvent-resistant nanofiltration

ABSTRACT

Bimetallic gold–palladium clusters, with an average size of 1.9 nm and composed of 80 mol% gold, proved to be highly active and selective metal catalysts for the organic phase oxidation with O_2 of aliphatic, allylic and benzylic alcohols to the corresponding carbonyl products. Polyvinylpyrrolidone stabilized gold–palladium clusters dispersed in *N*,*N*-dimethylformamide emerged as promising quasihomogeneous metal catalysts for the oxidation of benzyl alcohol to benzaldehyde with full selectivity; they could be efficiently recycled with unaffected catalytic performance by solvent-resistant nanofiltration. Highly active and durable heterogeneous catalysts for the amide phase or solvent-free alcohol oxidation were prepared by the quantitative immobilization of the optimized gold–palladium clusters on the high surface area basic $BaAl_2O_4$ spinel support with preservation of the bimetallic clusters' nanodispersion.

1. Introduction

The selective oxidation of alcohols to carbonyl compounds is a key transformation which is omnipresent in the production of fine and specialty chemicals [1,2]. Traditionally, alcohol substrates are oxidized by stoichiometric amounts of costly oxidants such as chromate or permanganate, inevitably resulting in the formation of environmentally unfriendly by-products [3]. An alternative, more ecological method involves the use of molecular O_2 or H_2O_2 as the oxidant in the presence of a catalyst, with water as the non-noxious co-product [4,5].

Both homogeneous and heterogeneous catalysts have been successfully applied in liquid phase alcohol oxidations [6]. Efficient homogeneous catalysts based on cobalt [7,8], copper [9,10], palladium [11–16] and ruthenium [17,18] have been reported. With respect to heterogeneous catalysts other than metal-based systems, heteropolyacids [19,20], hydrotalcites [21,22], mixed oxides [23–25] and molecular sieves [26] have been studied as oxidation catalysts.

Regarding heterogeneous metal catalysts, mostly palladium and platinum catalysts, either unpromoted or promoted by bismuth or lead, have widely been investigated despite the drawback of their sensitivity to deactivation as a consequence of surface overoxidation and chemical poisoning [27–30]. Conversely, for the gas phase oxidation of alcohols, the suitability of heterogeneous silver catalysts has been demonstrated [31–34].

Recently, the application of monometallic and bimetallic gold based catalysts in the liquid phase alcohol oxidation has been successfully explored. The beneficial role of gold is related to an enhanced rate and selectivity of the oxidation and moreover to an improved resistance to catalyst deactivation [35–51].

In this work, first the cluster size dependency of the oxidation activity will be studied in the amide phase oxidation of benzyl alcohol over polyvinylpyrrolidone stabilized Au clusters. Next, the doping of colloidal Au clusters with other metals will be investigated to enhance the catalytic performance. Subsequently,

* Corresponding author. Tel.: +32 16 32 16 39; fax: +32 16 32 19 98.
E-mail address: Dirk.DeVos@biw.kuleuven.be (D.E. De Vos).

1381-1169/$ – see front matter © 2009 Elsevier B.V. All rights reserved.
doi:10.1016/j.molcata.2009.07.017

the recycling of the best quasihomogeneous bimetallic catalyst is attempted by means of solvent-resistant nanofiltration (SRNF). Then, the immobilization of the optimized Au–Pd clusters on basic oxide supports is studied. Finally, the best heterogeneous Au–Pd catalyst will be applied in both the amide phase and solvent-free oxidation of various alcohols and the recyclability of the immobilized Au–Pd clusters will be assessed.

2. Experimental

2.1. Catalyst preparation

The metal (Me) colloids were synthesized by the addition of the appropriate amount of one or two metal chloride salts ($MeCl_x$: AgCl, $AuCl_3$, $PdCl_2$, $PtCl_4$; Sigma–Aldrich), leading to a total Me content of 0.1 mmol, to 8 mL of a stirred *N*,*N*-dimethylformamide (DMF) solution containing 0.111, 0.222, 0.333, 0.444, 0.555, 0.666, 0.777, 0.888, 0.999, 1.110, 1.221 or 1.332 g polyvinylpyrrolidone (PVP, MW = 10,000; Sigma–Aldrich). The applied variations in PVP concentration led to molar ratios of monomeric vinylpyrrolidone to total Me content of 10, 20, 30, 40, 50, 60, 70, 80, 90, 100, 110, 120 respectively. After 12 h stirring at 298 K, 2 mL of a DMF solution containing 0.4 mmol of dissolved $NaBH_4$ was added while stirring the solution (molar ratio $NaBH_4/MeCl_x = 4$) to generate the Me sol.

Immobilization of the Me colloids was attempted by the addition of 0.5 mL of an as-prepared Me sol to a 0.5 mL DMF volume containing 0.200 g of well-suspended powder support. Next this mixture was stirred for 12 h and this heterogenization procedure resulted in a Me loading of 25 μmol Me/g support in case of quantitative Me immobilization.

In order to partially remove excess PVP from the supported Me catalyst, the obtained amidic 1 mL suspension containing the oxide powder loaded with immobilized metal clusters was first isolated by centrifugation. After removal of the supernatant, 1 mL of DMF was added and the metal loaded powder was resuspended by stirring for 15 min and thereafter the powder fraction was isolated again by centrifugation. Additional catalyst washings were performed likewise.

Various oxide powders were used as supporting materials, such as γ-Al_2O_3, $MgAl_2O_4$, $CaAl_2O_4$, $SrAl_2O_4$, $BaAl_2O_4$, HSA-$MgAl_2O_4$, HSA-$CaAl_2O_4$, HSA-$SrAl_2O_4$, HSA-$BaAl_2O_4$, CeO_2, TiO_2, $BaTiO_3$, $CaTiO_3$, $MgTiO_3$ and $SrTiO_3$. HSA stands for high surface area. All supports were prepared according to literature procedures [52–54] except for γ-Al_2O_3, CeO_2 and TiO_2 which were supplied by Sigma–Aldrich.

For the co-precipitation preparation of the barium aluminate spinel ($BaAl_2O_4$) support the pH of an aqueous mixture of $Ba(NO_3)_2{\cdot}6H_2O$ and $Al(NO_3)_3{\cdot}9H_2O$ (stoichiometric ratio of $Ba^{2+}/Al^{3+} = 0.5$) was adjusted to 9.5 with an aqueous 30% ammonia solution. This solution was then stirred for 1 h and ripened overnight. The obtained precipitate was subsequently washed with de-ionized H_2O and thereupon dried for 15 h at 393 K. Finally, the resulting powder was calcined for 5 h at 1073 K leading to the formation of pure $BaAl_2O_4$ spinel.

The high surface area barium aluminate spinel (HSA-$BaAl_2O_4$) support was synthesized according to the sol–gel method proposed by Guo et al. [53]. To a stoichiometric aqueous solution of metal nitrates ($Ba(NO_3)_2{\cdot}6H_2O$, $Al(NO_3)_3{\cdot}9H_2O$) polyvinyl alcohol polymers (PVA, MW = 13,000–23,000; Sigma–Aldrich) were added. The molar ratio of metal ions to monomeric vinylalcohol was 0.2. The pH of the resulting viscous liquid was adjusted to 10 with the aqueous 30% ammonia solution. The suspension was then stirred for 3 h and aged overnight. Next, the precipitate was washed and dried for 15 h at 393 K. Finally, the obtained powder was calcined for 5 h at 1073 K.

2.2. Catalyst characterization

By X-ray diffraction (XRD) the crystallinity and crystal structure of the prepared oxide supports were studied as such directly after synthesis. The Brunauer–Emmett–Teller (BET) surface of the various oxides was determined by N_2 sorption measurements. Before sorption analysis, the powder samples were dried under N_2 flow for 6 h at 423 K. By Fourier transform infrared (FT-IR) spectroscopy the presence of surface hydroxyl groups on the oxide powders was verified in the 3200–3800 cm^{-1} range. Prior to pelletization the oxide supports were dried at 473 K in a vacuum oven for 6 h. To determine the basic properties of the oxide supports, 0.20 g of powder support was dried at 423 K for 6 h and thereafter suspended in 2 mL of an indicator solution (0.1 mg of bromothymol blue per mL of water-free toluene). These mixtures were stirred for 1 h and subsequently titrated with a 0.01 M solution of benzoic acid in toluene.

The monometallic Au sols were characterized by UV–Vis spectroscopy to detect the surface plasmon resonance (SPR) band which is conclusive evidence for the presence of Au as zerovalent nanoparticles. Moreover cluster size variations between the various Au nanocolloids can be observed by the shift in SPR wavelength position in the absorption spectrum [55,56]. The colloidal and immobilized Me clusters were characterized by transmission electron microscopy (TEM) at 200 kV. A droplet of a diluted Me sol or a drop of a well-homogenized solid Me catalyst suspension was dried on a carbon film supported by a copper grid. The mean Me cluster size was estimated as the mean diameter (d_p) for an ensemble of 200 particles. For each Me sol, the composition of 20 individual metal clusters on the copper grid was determined by energy dispersive X-ray (EDX) spot analysis during TEM characterization. Additionally 0.1 mL of a Me sol was immobilized on a glass plate to permit characterization by means of X-ray photoelectron spectroscopy (XPS) with a monochromated 450 W Al Kα source. The heterogeneous Me catalysts were subjected to thermogravimetric analysis (TGA) in O_2 to obtain information on the amount of PVP retained on the Me catalyst powder. Prior to TGA, the supported Me catalysts were dried for 24 h at 473 K under vacuum. The TGA temperature program started at 303 K up to 873 K with a 5 K/min increase. The PVP polymer typically burned off between 513 and 593 K. The efficiency of the Me immobilization and the degree of Me leaching from the supported Me catalysts in the oxidation experiments were investigated by inductively coupled plasma atomic emission spectrophotometry (ICP-AES), with a detection limit below 1 ppm for Au (267.6 nm) and Pd (340.5 nm).

2.3. Oxidation experiments and analysis

A typical reaction mixture for the amide phase alcohol oxidations with the quasihomogeneous Me catalysts consisted of 0.6 mL DMF, 0.4 mL of Me sol (equivalent with 4 μmol of Me) and 4 or 8 mmol of alcohol substrate (S), leading to molar S/Me ratios of 1000 and 2000.

For the amide phase oxidations with the heterogeneous Me catalysts the initial mixture consisted of 4.9 mL DMF, a 0.1 mL DMF volume of the well-suspended Me catalyst powder (equivalent with 0.5 μmol Me) and amounts of alcohol substrate varying between 0.25 and 25 mmol. This results in molar S/Me ratios between 500 and 50,000.

For the solvent-free oxidations, 0.2 mL of the DMF suspension of the supported Me catalyst (1 μmol Me) diluted by 0.8 mL DMF was centrifugated to isolate the solid fraction. Fivefold washing of the catalyst with 1 mL volumes of DMF was performed as described above. Next, the residual DMF was removed by resuspending the precipitated metal catalyst in 2.44 g 1-phenylethanol (20 mmol) and isolating the catalyst by centrifugation (7500 rpm, 15 min). This

solvent exchange procedure was repeated four times. After the fifth catalyst washing and final resuspension in 6.11 g 1-phenylethanol (50 mmol) the mixture is ready for the oxidation with a S/Me ratio of 50,000.

The reaction mixtures were pressurized to 0.2–4.0 MPa O_2 and kept at 353–433 K while stirring at 1000 rpm for different reaction times (r.t.). The oxidations applying the quasihomogeneous Me catalysts were performed in a high-throughput mode by means of a multi-reactor unit (TOP Industrie, France) containing 10 mini-reactors, while the oxidations with the heterogeneous Me catalysts and all recycling experiments were carried out in thermocontrolled autoclaves. All oxidation experiments were performed in triplicate for statistical reliability. The differences in catalytic activity for comparable oxidation runs were always below 3% while no variations were detected for the oxidation selectivity. Blank experiments in the absence of the Me catalysts were performed to evaluate potential product formation as a result of autoxidation. No oxidation products were detected in the blank experiments by gas chromatography (GC) analysis.

For the experimental data analysis, a FID equipped GC was used with a WCOT fused silica column coated with a Chrompack CP-WAX 58 CB stationary phase. The retention times of potential oxidation products were compared with those of the commercial reference compounds. Peak assignment was aided by gas chromatography–mass spectrometry (GC–MS) analysis of the reaction samples. The average turnover frequency (TOF_{av}, h^{-1}) represents the molar ratio of converted substrate vs. metal, divided by the reported reaction time, and is thus an appropriate measure for the average catalytic activity of the Me catalysts.

2.4. Catalyst recycling experiment

The recycling experiments with quasihomogeneous Me catalysts comprised of five successive oxidation runs, with four membrane filtrations in between. The phase-inversion synthesis of the SRNF membrane, the post-synthesis modification and the physicochemical characterization have previously been described [57]. The filtrations by means of the cross-linked asymmetric polyimide (PI) membranes were performed at ambient temperature applying a driving force of 1.0 MPa N_2. An autoclave was filled with 6 mL DMF, 4 mL of Me sol and 80 mmol of benzyl alcohol (leading to S/Me ratio of 2000), after which the autoclave was pressurized to 2.0 MPa O_2 at 373 K for 1 h. After this first oxidation run, the composition of the reaction mixture was determined by removing an aliquot for GC analysis. The remainder present in the filtration cell was concentrated by SRNF to a 4 mL DMF volume containing the colloidal Me catalyst. This Me sol volume was washed twice with 10 mL DMF until a total filtrate volume of 26 mL had been collected. The retained volume was analyzed by GC to verify the absence of benzyl alcohol and benzaldehyde. The recycled colloidal Me dispersion was diluted with 6 mL DMF and this amide volume was considered as the starting mixture for the second oxidation run after addition of 80 mmol benzyl alcohol. The same procedure was followed for the further filtration and reuse experiments. The recycling experiments with the quasihomogeneous Me catalysts were performed in threefold.

The Me retention by the PI membrane was determined by means of ICP-AES. To assess the deposition of the Me colloids on the membrane surface during the filtration experiments, the PI membrane was first applied in a Me sol filtration after which 1 cm^2 membrane was digested in 2 mL of *aqua regia*, which was then analyzed by ICP-AES.

For the recycling of the heterogeneous Me catalysts in DMF, the Me catalyst (0.5 μmol Me) was separated from the reaction mixture via centrifugation and the supernatant was removed for analysis. Next, the Me catalyst powder was washed for five times (resuspending in 5.0 mL DMF followed by centrifugation). After addition of 5.0 mL DMF and 1.08 g benzyl alcohol a next run was started.

For the recycling experiments with the heterogeneous Me catalysts in solvent-free oxidations, the reaction mixtures were centrifuged after which the supernatant was removed for analysis. Thereupon the deposited heterogeneous Me^0 catalyst powder was washed five times with 2.44 g 1-phenylethanol. A successive oxidation experiment was started by addition of 6.11 g 1-phenylethanol. These recycling experiments were likewise performed in triplicate.

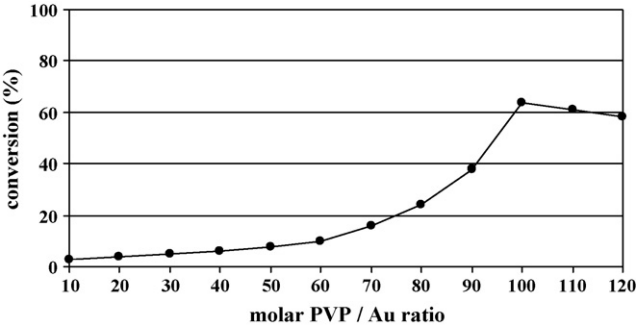

Fig. 1. Benzyl alcohol oxidation: conversion as a function of the synthesis PVP/Au ratio of the quasihomogeneous Au^0 catalyst. Conditions: DMF, benzyl alcohol/Au = 1000, 373 K, 2.0 MPa O_2, 1 h.

3. Results and discussion

3.1. Oxidations with quasihomogeneous Me^0 catalysts

Firstly, PVP stabilized Au clusters dispersed in DMF were prepared by hydride reduction, with varying PVP/Au ratios at constant Au content. XPS confirmed that all Au species present in the prepared Au sols were in the metallic state as the $Au4f_{7/2}$ level was detected at a binding energy of 84.0 eV [57]. The variations in stabilization by PVP resulted in different Au cluster size distributions for the generated Au^0 colloids as revealed by UV–Vis spectroscopy and TEM [57]. The Au^0 sols synthesized with molar PVP/Au ratios ≥100 displayed a reddish brown color and a distinct SPR band could not be discerned in the corresponding UV–Vis spectra. Conversely, for the more reddish Au^0 sols generated with molar PVP/Au ratios <100, distinct SPR bands were observed and the wavelength positions of the SPR maximum varied between 515 and 530 nm. The actual dimensions of the colloidal Au^0 clusters determined via TEM ranged between 1.8 (PVP/Au = 100) and 6.2 nm (PVP/Au = 10). For the Au^0 colloids generated with molar PVP/Au ratios ≥100 no clear difference in mean Au cluster size could be discerned compared to the Au^0 clusters prepared with a PVP/Au ratio of 100 (d_p = 1.8 nm).

The Au^0 nanocolloids, each with a characteristic cluster size, were evaluated as quasihomogeneous metal catalysts in the benzyl alcohol oxidation in DMF (373 K and 2.0 MPa O_2). Remarkably, addition of an extra base was not required to attain high oxidation rates in contrast with earlier reports on the promotion of nano-Au^0 by inorganic bases like NaOH and K_2CO_3 [50,58]. The basic functional groups in the reaction medium (DMF) and the protective polymer (PVP) clearly are sufficient as promoters. Moreover, complete product selectivity to benzaldehyde was observed. Frequently observed by-products such as benzoic acid as well as condensation products like benzyl benzoate could not be retrieved from the product pool by GC–MS analysis of the reaction samples [58–60].

The data in Fig. 1 point to the dependency of the turnover rate on the mean Au cluster size of the different Au^0 nanocolloids [47,61]. The Au^0 colloids, with a molar PVP/Au ratio of 100 and with a mean d_p of 1.8 nm, emerged as the most active colloidal Au^0 catalysts with an average turnover frequency of 630 h^{-1} after a 1 h reaction time

Table 1
XPS characterization of bimetallic Au–Pd catalysts.

Catalyst	$Au4f_{7/2}$ (eV)	$Pd3d_{5/2}$ (eV)
Own Au–Pd catalyst	84.0	335.8
Au–Pd catalyst [62]	84.0	335.3
Au–Pd catalyst [63]	83.9	335.2

in the benzyl alcohol oxidation. The Au^0 nanocolloids with similar cluster dimensions, but synthesized with a higher PVP content ($120 \geq PVP/Au > 100$), were slightly less active (at most 6%) than the optimum colloidal Au^0 catalyst. This activity decline may be ascribed to increased diffusion limitation around the Au^0 clusters and blocking of catalytic sites on the Au^0 surface by excess PVP. Conversely, the lower activity of the Au^0 nanocolloids generated with less PVP protection ($PVP/Au < 100$) is related to the reduced metal dispersion of the corresponding Au^0 clusters as a result of the diminished level of sterical and polar stabilization by PVP during the Au^0 sol synthesis.

Next, the effect of doping the optimized Au^0 nanocolloids with Ag, Pd and Pt species was evaluated in view of the proven suitability of these metals as oxidation catalysts [27–34], and the recently proposed synergetic effect between Au and Pd [39,60]. For that purpose, monometallic colloids (Au, Ag, Pd and Pt) and bimetallic colloids (Au–Ag, Au–Pd, Au–Pt) were synthesized in DMF. The molar PVP/Me ratio was in each case 100 and for the bimetallic sols, an equimolar composition of both metals (molar ratio $Me_1/Me_2 = 5{:}5$) was used. For the Me^0 sols containing Ag and Pt, no enhancement of the oxidation activity was observed in comparison with the monometallic Au^0 sols. Only the colloidal (5:5) Au–Pd catalyst showed an advantageous effect of addition of a second metal to Au in the benzyl alcohol oxidation. This bimetallic catalyst led to a significantly increased oxidation rate ($TOF_{av} = 1180\ h^{-1}$) with unaffected oxidation chemoselectivity in comparison with its monometallic Au counterpart. The (5:5) Au–Pd clusters displayed a narrow size distribution and measured on average 2.1 nm. Therefore the enhanced oxidation rate could not be ascribed to an increase in metal dispersion.

XPS revealed that the bimetallic Au–Pd sol consisted of zerovalent Au and Pd atoms as the $Au4f_{7/2}$ and $Pd3d_{5/2}$ binding energy levels were observed at, respectively, 84.0 eV and 335.8 eV (Table 1) [62,63]. EDX spot analysis pointed out that the Au^0–Pd^0 nanosol consisted of bimetallic Au–Pd clusters [64]. However, it proved impracticable to discern a difference between the surface and bulk Au/Pd ratios for the Au^0–Pd^0 clusters as a consequence of their high dispersion.

Next Au^0–Pd^0 nanocolloids with varying Au/Pd ratios ($PVP/Me = 100$) were synthesized to determine the optimum composition maximizing the benzyl alcohol oxidation rate. As reported in Fig. 2, a molar synthesis Au/Pd ratio of 8:2 resulted in the highest TOF_{av} value ($1920\ h^{-1}$) and a preserved full benzaldehyde selectivity.

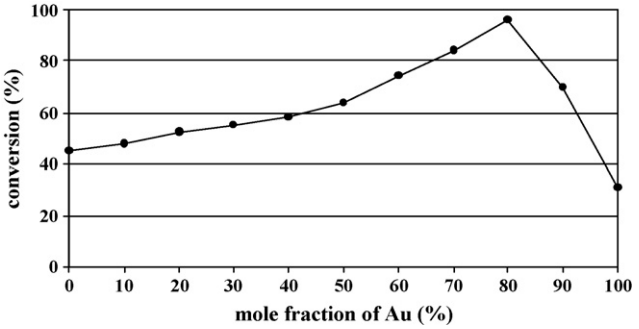

Fig. 2. Benzyl alcohol oxidation: conversion as a function of the synthesis Au/Pd ratio of the quasihomogeneous Au^0–Pd^0 catalyst. Conditions: DMF, $PVP/Me = 100$, benzyl alcohol/$Me = 2000$, 373 K, 2.0 MPa O_2, 1 h.

The optimized (8:2) Au^0–Pd^0 clusters measured 1.9 nm (Fig. 3a). Calculations on the EDX spot analysis of individual metal clusters pointed out that the optimum (8:2) Au^0–Pd^0 sol consisted of uniform clusters containing 80.5 mol% Au and 19.5 mol% Pd, which strongly resembles to the Au/Pd ratio of the bimetallic sol synthesis. This observation demonstrates that both the cluster size and composition can be controlled during synthesis of the bimetallic sol, by the ratios of PVP/(Au + Pd) and Au/Pd respectively. The most appropriate Au/Pd composition moreover strongly resembles the reported optimized composition (molar Au/Pd ratio of 9:1) of a Au–Pd catalyst for the glycerol oxidation [65].

The molar PVP/Me ratio of 100 was confirmed as the most appropriate proportion of stabilization for the (8:2) Au^0–Pd^0 colloids as well. The monometallic Pd^0 colloids, also showing a full selectivity to benzaldehyde, displayed a TOF_{av} value of $910\ h^{-1}$ and had a mean cluster size around 2.4 nm, while the optimum Au^0 colloids ($d_p \cong 1.8$ nm) led to a TOF_{av} value of $620\ h^{-1}$ under the reaction conditions defined in Fig. 2. Therefore the better performance of the quasihomogeneous Pd^0 catalyst in comparison with its pure, Au based counterpart, with a higher metal dispersion, must be related to an intrinsically higher oxidation activity of Pd versus Au.

At this stage, it was attempted to recycle the optimum (8:2) Au^0–Pd^0 nanocolloids from the amidic reaction medium by solvent-resistant nanofiltration (SRNF). In previous work a polymeric membrane with a superior durability in demanding media like DMF has been introduced [66]. This asymmetric polyimide (PI) membrane, prepared via the phase-inversion technique and modified by a post-synthesis chemical cross-linking, proved highly effective for the separation of PVP stabilized Ag^0 clusters ($d_p \cong 4.2$ nm). Characterization of the cross-linked PI membrane revealed that the substitution of imidic bonds by amidic bonds made the membrane chemically stable in amidic and aromatic media [57]. By use of this custom-made SRNF membrane for the recycling of the (8:2) Au^0–Pd^0 nanocolloids from the reaction medium, a Me retention exceeding 99.5% was achieved; ICP-AES analysis of a used membrane fragment dissolved in *aqua regia*, revealed the absence of Me deposition on the membrane surface. The recycled (8:2) Au^0–Pd^0 nanocolloids preserved at least 95% of the inceptive oxidation activity in the fifth benzyl alcohol oxidation run with a fully preserved benzaldehyde selectivity (373 K and 2.0 MPa O_2). This observation demonstrates the stable performance of the bimetallic nanocolloids as quasihomogeneous metal catalysts and thus their robust physicochemical nature.

3.2. Oxidations with heterogeneous Au^0–Pd^0 catalysts

Secondly, it was attempted to immobilize the Au^0–Pd^0 nanocolloids with optimized size and composition on metal oxide powders of which the suitability as supports for oxidation metal catalysts has been proven before (γ-Al_2O_3, CeO_2, TiO_2) or of which the basic properties were expected to be beneficial for the activity promotion of the bimetallic clusters (basic spinel and perovskite structures) [48,59,67]. The objective of this immobilization was threefold: firstly to promote the catalytic performance of the optimized Au^0–Pd^0 clusters, secondly to generate a heterogeneous metal catalyst thereby simplifying the recycling and thirdly to enable application in solvent-free conditions.

The immobilization of the optimum bimetallic clusters on γ-Al_2O_3, CeO_2 and TiO_2, aiming at a total Me loading of 0.025 mmol or $\cong 0.005$ g per gram of support, was expected to be quantitative considering the low metal loading and the strong affinity of the PVP stabilizer for hydroxyl groups. The presence of surface hydroxyls on all supports was confirmed by FT-IR spectroscopy as found before [68–70]. Adsorption of the PVP polymers, stabiliz-

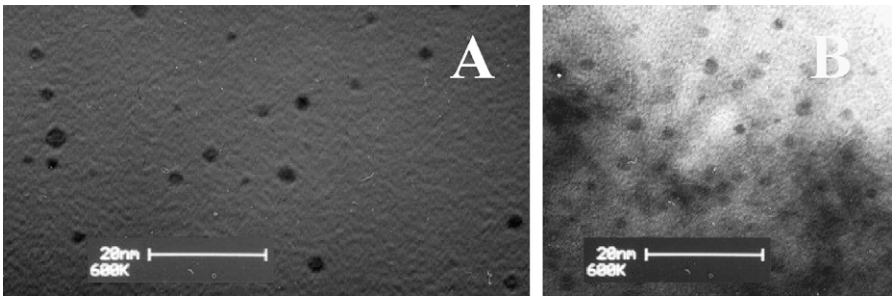

Fig. 3. (a) TEM picture of quasihomogeneous (8:2) Au^0–Pd^0 catalyst; (b) TEM picture of heterogeneous (8:2) Au^0–Pd^0/HSA-$BaAl_2O_4$ catalyst.

ing the (8:2) Au^0–Pd^0 clusters, on the metal oxide supports occurs through hydrogen bonding or via acid–base interactions with the surface hydroxyl groups [71,72]. The γ-Al_2O_3 support had a specific BET area of 112 m^2/g which was significantly higher than the ceria support (34 m^2/g) and the titania support (16 m^2/g). As a consequence of the differences in specific surface area and thus of the number of hydroxyl adsorption sites, only for the γ-Al_2O_3 support complete heterogenization of the bimetallic clusters was obtained, which contrasts with CeO_2 and TiO_2 for which metal immobilization was not complete, as in the case of γ-Al_2O_3 after prolonged centrifugation no bimetallic nanocolloids could be retrieved in the supernatant and element analysis of the supernatant proved the absence of Au or Pd species in the supernatant. The ICP-AES detection limit of 1 ppm enabled to detect the potential presence in the supernatant of less than 0.01% of the total amount of Au and Pd.

After resuspending the support powders, whether with quantitatively deposited (8:2) Au^0–Pd^0 clusters or not with a fraction of the bimetallic clusters remaining in the colloidal state in the case of the CeO_2 and TiO_2 supports, the benzyl alcohol substrate was added and next the mixtures were subjected to standard oxidation conditions. As all three supports contain basic sites with comparable strengths [68,73,74], only a different number of basic surface sites interacting with the bimetallic clusters can account for the differences in base promotion. Only for the γ-alumina supported Au^0–Pd^0 clusters a marked increase in oxidation rate and thus a true promoting support effect was found. These observations can be rationalized in terms of the incomplete deposition of the bimetallic clusters on the ceria and titania supports which implies that a substantial fraction of the bimetallic clusters, which remained in the colloidal state, could not be promoted on the supporting oxide surface. The superiority of the γ-alumina support was thus a result of its high surface area which enabled complete immobilization of the bimetallic clusters and thus the highest number of basic sites interacting with the Au^0–Pd^0 clusters. The promoting effect of the alumina support was however limited, with a benzyl alcohol turnover frequency of 2070 h^{-1}. This represents an increase in oxidation rate of only 8% in comparison with the results obtained with the quasihomogeneous (8:2) Au^0–Pd^0 catalyst under the same application conditions (373 K and 2.0 MPa O_2).

In view of the recent successes with oxides containing group II metals (e.g. $Mg_3Al_1O_x$) as supports for Au based oxidation catalysts, the use of aluminate spinel supports containing Mg, Ca, Sr and Ba has been investigated [75]. The XRD reflections of all prepared spinel supports could be assigned to the spinel phases, without detection of alumina or other metal oxides (Fig. 4).

For all aluminate spinel structures, apart from a complete immobilization of the bimetallic clusters, a more substantial promotion was found compared to the γ-alumina support, with a gradual increase in benzyl alcohol oxidation rates from $MgAl_2O_4$ over $CaAl_2O_4$ and $SrAl_2O_4$ to $BaAl_2O_4$. The observed average oxidation rates progressively varied between 2210 h^{-1} for $MgAl_2O_4$ and

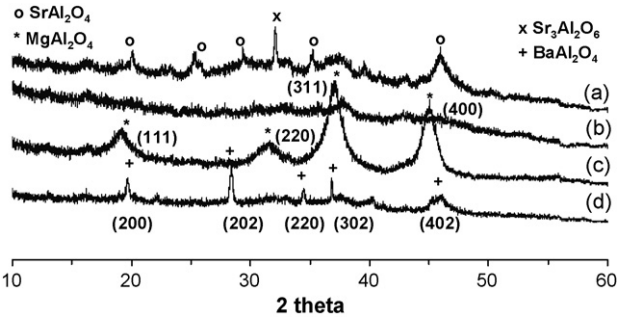

Fig. 4. XRD analyses of $SrAl_2O_4$ (a), $CaAl_2O_4$ (b), $MgAl_2O_4$ (c) and $BaAl_2O_4$ (d) spinel supports.

2380 h^{-1} for $BaAl_2O_4$, which corresponds to further improvements of the bimetallic clusters' activity ranging from 15% to 24% in comparison with the unsupported (8:2) Au^0–Pd^0 colloids (Table 2).

To gain more insight into differences between the supported catalysts, the surface areas of the different aluminate spinels were determined by N_2 sorption. The dispersion of the Sr aluminate (175 m^2/g) proved higher than that of the Ba aluminate (154 m^2/g) and the Ca aluminate (150 m^2/g) while the Mg aluminate support had a surface area of only 106 m^2/g. Obviously the variations in surface area cannot be the sole support variable accounting for the differences in base promotion.

To further elucidate the differences between the catalysts, the basicity of the individual supports was determined as the basic properties of the supports were presumably significant for the catalytic activity. The supports' basicity was determined by acid titration with bromothymol blue (pK_a = 7.1) as the pH indicator [78,79]. The titrated number of basic sites amounted to 0.22 mmol/g for $MgAl_2O_4$, 0.38 mmol/g for $CaAl_2O_4$, 0.53 mmol/g for $SrAl_2O_4$ and 0.64 mmol/g for $BaAl_2O_4$. In view of the analogous trend in determined number of basic sites and observed oxidation rates, the variations in support promotion can in our opinion be ascribed to the different number of basic sites. Therefore, the superiority of the Ba aluminate as a promoting support can be explained by the higher content of basic surface sites in comparison with the other aluminate spinel supports.

In subsequent attempts to enhance the support promotion, firstly analogous aluminate spinel supports have been prepared via

Table 2
Benzyl alcohol oxidation in DMF over heterogeneous (8:2) Au^0–Pd^0 catalysts.

Support	BET surface (m^2/g)	Titrated basicity (mmol/g)	TOF_{av} (h^{-1})
$MgAl_2O_4$	106	0.22	2210
$CaAl_2O_4$	150	0.38	2310
$SrAl_2O_4$	175	0.53	2360
$BaAl_2O_4$	154	0.64	2380

Conditions: DMF, 373 K, 2.0 MPa O_2, S/Me = 2000, 45 min.

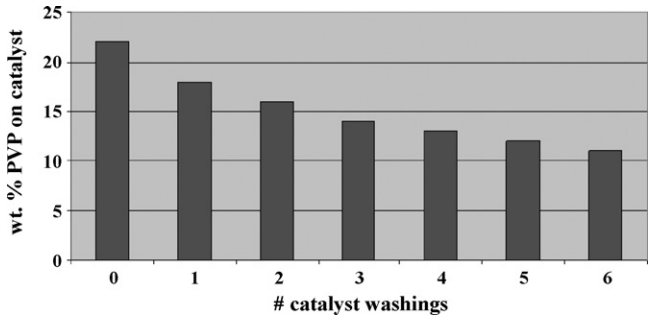

Fig. 5. PVP removal as a function of number of catalyst washings.

an alternative synthesis procedure, leading to even higher surface areas. For the high surface analogue of the most appropriate support, i.e. HSA-$BaAl_2O_4$, a surface area of 229 m^2/g was achieved. As a result of the higher contact area for the bimetallic clusters, an improvement of about 5% in benzyl alcohol oxidation rate was obtained with the 0.5 wt% (8:2) Au^0–Pd^0/HSA-$BaAl_2O_4$ catalyst compared to the analogous (8:2) Au^0–Pd^0 catalyst with the regular Ba aluminate support, which resulted in an average turnover rate of 2490 h^{-1} under the standard reaction conditions.

These successful aluminate supports were compared with regular oxide (MeO) and perovskite ($MeTiO_3$) type supports based on Mg, Ca, Sr and Ba. With these non-spinel supports, the immobilization of the (8:2) Au^0–Pd^0 clusters was incomplete, and no promoting effect could be observed. This can be ascribed to the low surface areas (7–31 m^2/g). A similar superiority of the spinel supports over the corresponding regular oxides has been found before for Au catalysts in CO oxidation [76,77].

Inspired by earlier findings on the beneficial effect of PVP removal on the catalytic performance of supported metal clusters, it was attempted to further enhance the catalytic activity by partially removing the PVP polymers from the HSA-$BaAl_2O_4$ support [80]. This can be achieved, without loss of Au^0–Pd^0 clusters, by rinsing the optimized heterogeneous (8:2) Au^0–Pd^0 catalyst with DMF. This should improve the contact of the basic support with the catalytic metal clusters without affecting their nanodispersion. The PVP removal as a consequence of the successive washings was determined by TGA while the potential metal leaching was monitored by ICP-AES. Fivefold washing resulted in a decrease of the PVP adsorbed on the HSA-$BaAl_2O_4$ support from 22 to 12 wt% (Fig. 5). An additional catalyst washing further reduced the PVP content but some release of Au^0–Pd^0 clusters was observed and therefore further rinsing steps were omitted.

Application of the obtained 0.5 wt% (8:2) Au^0–Pd^0/HSA-$BaAl_2O_4$ with reduced PVP content under standard conditions (2.0 MPa O_2 and 373 K) resulted in a TOF_{av} of 2680 h^{-1} in the benzyl alcohol oxidation, which corresponds to an activity increase of about 8% in comparison with the analogous non-washed heterogeneous catalyst. A TEM picture of the optimized heterogeneous bimetallic catalyst is represented in Fig. 3b, and the comparison of the mean particle size of the quasihomogeneous and heterogeneous bimetallic clusters confirmed that the heterogenization of the bimetallic clusters proved possible without loss of metal nanodispersion.

Comparing the turnover rates in the benzyl alcohol oxidation obtained with the quasihomogeneous (TOF_{av} = 1920 h^{-1}) and the optimized heterogeneous (TOF_{av} = 2680 h^{-1}) (8:2) Au^0–Pd^0 catalyst reveals that the basic promotion by immobilization led to a 40% increase in oxidation rate. This comparison evidences that the heterogenization approach of the active catalytic phase is truly worthwhile, as not only the catalyst recycling is simplified, but also the intrinsically promising activity of the (8:2) Au^0–Pd^0 clusters is further improved.

Table 3
Temperature effect on amide phase oxidation of benzyl alcohol over (8:2) Au^0–Pd^0/HSA-$BaAl_2O_4$.

Temperature (K)	S/Me (mol/mol)	Time (min)	C (%)	TOF_{av} (h^{-1})	S (%)
353	1000	60	99	990	100
373	2500	55	98	2680	100
393	7500	55	93	7640	100
413	20,000	60	99	19,970	100
433	50,000	55	97	53,060	96

Conditions: DMF, 2.0 MPa O_2, time = reaction time, S = selectivity to benzaldehyde.

After optimization of the catalyst, the effect of the reaction variables O_2 pressure (0.2–4.0 MPa) and temperature (353–433 K) was investigated in the amide phase oxidation of benzyl alcohol to determine the optimal reaction conditions. It was found that the optimum O_2 pressure was 2.0 MPa, as higher O_2 pressures (4.0 MPa) did not result in a distinct increase in oxidation rate (only 4%). Lower O_2 pressures on the other hand led to lower oxidation rates, for example a decrease of 11% from 2.0 to 0.2 MPa O_2. Conversely, the reaction temperature had a more pronounced effect on the oxidation rate, with a strong increase up to 413 K combined with a preserved complete selectivity to benzaldehyde (Table 3). At 413 K and 2.0 MPa O_2, a TOF_{av} of 19,970 h^{-1} was found in the benzyl alcohol oxidation over the (8:2) Au^0–Pd^0/HSA-$BaAl_2O_4$ catalyst. At higher reaction temperatures, e.g. 433 K, an oxidation rate of 53,060 h^{-1} was observed but the selectivity to benzaldehyde was no longer complete as a consequence of limited overoxidation and decarboxylation to benzene. Even under these high temperature conditions, no release of bimetallic clusters from the HSA powder support was found as determined by ICP-AES. For the further alcohol oxidations in DMF, the applied reaction variables will be 413 K and 2.0 MPa O_2.

The optimized (8:2) Au^0–Pd^0/HSA-$BaAl_2O_4$ catalyst was applied in the amide phase oxidation of a series of benzylic, allylic and aliphatic alcohols to the corresponding aldehydes and ketones. This approach provided the opportunity to assess the applicability of the developed heterogeneous bimetallic catalyst and to investigate the dependency of the oxidation rate on the structure of the alcohol substrate.

As shown in Table 4, the secondary alcohols displayed a higher reactivity compared to the primary alcohol substrates, and a decrease in alcohol reactivity was observed in the order benzylic > allylic > aliphatic. In all oxidation experiments a complete selectivity to the corresponding carbonyl compound was found. Markedly, also for aliphatic alcohol substrates considerable turnover rates were observed, with TOF_{av} values above 500 h^{-1}. The principal conclusion of Table 4 is that the (8:2) Au^0–Pd^0/HSA-$BaAl_2O_4$ catalyst is applicable to oxidation of a wide scope of alcohol substrates in amides.

Next, the (8:2) Au^0–Pd^0/HSA-$BaAl_2O_4$ catalyst has been evaluated in the solvent-free oxidation of 1-phenylethanol. A TOF_{av} value of 58,190 h^{-1} was found after 50 min reaction time, which stands for an increase of approximately 10% in comparison with the amide phase 1-phenylethanol oxidation under identical conditions

Table 4
Amide phase oxidation over (8:2) Au^0–Pd^0/HSA-$BaAl_2O_4$.

Substrate (S)	S/Me (mol/mol)	Time (min)	C (%)	TOF_{av} (h^{-1})
Benzyl alcohol	20,000	60	99	19,980
1-Phenylethanol	50,000	54	95	52,760
Crotyl alcohol	2,000	48	96	2,390
1-Octen-3-ol	2,000	66	94	1,710
3-Octanol	1,500	75	98	1,170
1-Octanol	500	45	94	630
1-Butanol	1,000	60	97	970

Conditions: DMF, 413 K, 2.0 MPa O_2.

Table 5
Recycling experiments with (8:2) Au^0–Pd^0/HSA-$BaAl_2O_4$.

Oxidation	Run	Time (min)	C (%)	TOF_{av} (h^{-1})
Benzyl alcohol oxidation in DMF[a]	1	60	99	19,910
	5	60	96	19,140
Solvent-free 1-phenylethanol oxidation[b]	1	50	97	58,020
	5	50	94	56,380

[a] Conditions: DMF, 413 K, 2.0 MPa O_2, S/Me = 20,000.
[b] Conditions: 1-phenyl-ethanol, 413 K, 2.0 MPa O_2, S/Me = 50,000.

(413 K and 2.0 MPa O_2) apart from the reaction medium. Performing the alcohol oxidation in solvent-free conditions is clearly not only ecologically benign, but also enhances the heterogeneous metal catalyst's activity.

Finally, the durability of the optimized heterogeneous Au^0–Pd^0 catalyst was assessed during recycling experiments on the benzyl alcohol oxidation in amide phase and on the 1-phenylethanol oxidation in solvent-free conditions, as reported in Table 5. Using element analysis, it was found that no Au, Pd, Ba or Al species were present in all supernatant phases obtained after separation of the heterogeneous catalyst. With the 1 ppm detection limit, an amount of leached Au, Pd, Ba or Al in the supernatant as low as 0.5% of the total content present in the heterogeneous catalyst could be detected for the recycling experiments. For both oxidations, it was found that in the fifth oxidation run more than 95% of the initial metal catalyst activity was maintained, with unaffected full selectivity to, respectively, benzaldehyde and acetophenone. These findings evidence the stable nature of the developed (8:2) Au^0–Pd^0/HSA-$BaAl_2O_4$ catalyst in both amidic and aromatic media.

4. Conclusion

Summarizing, the successful application of optimized Au^0–Pd^0 clusters both as quasihomogeneous and heterogeneous metal catalysts for the liquid phase alcohol oxidation has been demonstrated. The optimized (8:2) Au^0–Pd^0 nanocolloids not only emerged as stable and recyclable colloidal catalysts, but proved to be excellent precursors for the synthesis of supported metal catalysts. Optimization of the heterogenization of the (8:2) Au^0–Pd^0 clusters (d_p = 1.9 nm) by assessing various powder supports and by promoting the contact between the bimetallic clusters and the supporting material led to a heterogeneous (8:2) Au^0–Pd^0/HSA-$BaAl_2O_4$ catalyst. This catalyst was applicable to a wide substrate scope of alcohol types and displayed an excellent performance and recyclability via SRNF in the amide phase and solvent-free oxidation of alcohols. The marked support effect on the bimetallic clusters' catalytic performance is a result of the support's high surface area and basicity.

Acknowledgements

PGNM thanks K.U.Leuven for a postdoctoral fellowship grant. SLFC acknowledges IWT for a PhD scholarship. This research was done in the framework of an I.A.P.–P.A.I. grant (IAP 6/27) on Supramolecular Catalysis sponsored by the Belgian Federal Government, and of an excellence grant (CECAT) of K.U.Leuven.

References

[1] R.A. Sheldon, J.K. Kochi, Metal-Catalyzed Oxidations of Organic Compounds, Academic Press, New York, 1981.
[2] M. Hudlicky, Oxidations in Organic Chemistry, American Chemical Society, Washington DC, 1990.
[3] G. Cainelli, G. Cardillo, Chromium Oxidations in Organic Chemistry, Springer–Verlag, Berlin, 1984.
[4] R.A. Sheldon, I.W.C.E. Arends, A. Dijksman, Catal. Today 57 (2000) 157–166.
[5] R.A. Sheldon, I.W.C.E. Arends, G.J. ten Brink, A. Dijksman, Acc. Chem. Res. 25 (2002) 774–781.
[6] B.-Z. Zhan, A. Thompson, Tetrahedron 60 (2004) 2917–2935.
[7] T. Iwahama, S. Sakaguchi, Y. Nishiyama, Y. Ishii, Tetrahedron Lett. 36 (1995) 6923–6926.
[8] T. Iwahama, Y. Yoshino, T. Keitoku, S. Sakaguchi, Y. Ishii, J. Org. Chem. 65 (2000) 6502–6507.
[9] I.E. Marko, P.R. Giles, M. Tsukazaki, S.M. Brown, C.J. Urch, Science 274 (1996) 2044–2046.
[10] I. Marko, P.R. Giles, M. Tsukazaki, I. Chelle-Regnaut, A. Gautier, S.M. Brown, C.J. Urch, J. Org. Chem. 64 (1999) 2433–2439.
[11] B.A. Steinhoff, S.R. Fix, S.S. Stahl, J. Am. Chem. Soc. 124 (2002) 766–767.
[12] B.A. Steinhoff, S.S. Stahl, Org. Lett. 4 (2002) 4179–4181.
[13] T. Nishimura, Y. Maeda, N. Kaikiuchi, S. Uemura, J. Chem. Soc., Perkin Trans. 1 (2000) 4301–4305.
[14] T. Nishimura, T. Onoue, K. Ohe, S. Uemura, J. Org. Chem. 64 (1999) 6750–6755.
[15] G.J. ten Brink, I.W.C.E. Arends, R.A. Sheldon, Science 287 (2000) 1636–1639.
[16] G.J. ten Brink, I.W.C.E. Arends, R.A. Sheldon, Adv. Synth. Catal. 344 (2002) 355–369.
[17] I. Marko, P.R. Giles, M. Tsukazaki, I. Chelle-Regnaut, C.J. Urch, S.M. Brown, J. Am. Chem. Soc. 119 (1997) 12661–12662.
[18] M. Hasan, M. Musawir, P.N. Davey, I.V. Kozhevnikov, J. Mol. Catal. A 180 (2002) 77–84.
[19] W. Turek, M. Lapkowki, J. Debiec, A. Krowiak, Appl. Surf. Sci. 252 (2005) 847–852.
[20] M.M. Heravi, V. Zadsirjan, K. Bakhtiari, M.A. Oskooie, F.F. Bamoharram, Catal. Commun. 8 (2007) 315–318.
[21] S. Velu, N. Shah, T.M. Jyothi, S. Sivasanker, Micropor. Mesopor. Mater. 33 (1999) 61–75.
[22] V.R. Choudhary, D.K. Dumbre, B.S. Uphade, V.S. Narkhede, J. Mol. Catal. A 215 (2004) 129–135.
[23] F. Somma, G. Strukul, J. Catal. 227 (2004) 344–351.
[24] H.G. Manyar, G.S. Chaure, A. Kumar, J. Mol. Catal. A 243 (2006) 244–252.
[25] S.S. Deshpande, R.V. Jayaram, Catal. Commun. 9 (2008) 186–193.
[26] V.D. Makwana, L.J. Garces, J. Liu, J. Cai, Y.-C. Son, S.L. Suib, Catal. Today 85 (2003) 225–233.
[27] T. Mallat, A. Baiker, Catal. Today 19 (1994) 247–283.
[28] P. Gallezot, Catal. Today 37 (1997) 405–418.
[29] M. Besson, P. Gallezot, Catal. Today 57 (2000) 127–141.
[30] T. Mallat, A. Baiker, Chem. Rev. 104 (2004) 3037–3058.
[31] Z. Yang, J. Li, X. Xiangguang, X. Xie, Y. Wu, J. Mol. Catal. A 241 (2005) 15–22.
[32] R. Yamamoto, Y. Sawayama, H. Shibahara, Y. Ichihashi, S. Nishiyama, S. Tsuruya, J. Catal. 234 (2005) 308–317.
[33] Y. Sawayama, H. Sibahara, Y. Ichihashi, S. Nishiyama, S. Tsuruya, Ind. Eng. Chem. Res. 45 (2006) 8837–8845.
[34] J. Shen, W. Shan, Y. Zhang, J. Du, H. Xu, K. Fan, W. Shen, Y. Tang, J. Catal. 237 (2006) 94–101.
[35] W.C. Ketchie, M. Murayama, R.J. Davis, Top. Catal. 44 (2007) 307–317.
[36] W.C. Ketchie, Y.-L. Fang, M.S. Wong, M. Murayama, R.J. Davis, J. Catal. 250 (2007) 94–101.
[37] W.C. Ketchie, M. Murayama, R.J. Davis, J. Catal. 250 (2007) 264–273.
[38] C. Bianchi, F. Porta, L. Prati, M. Rossi, Top. Catal. 13 (2000) 231–236.
[39] N. Dimitratos, A. Villa, D. Wang, F. Porta, D. Su, L. Prati, J. Catal. 244 (2006) 113–121.
[40] N. Dimitratos, A. Villa, C.L. Bianchi, L. Prati, M. Makkee, Appl. Catal. A 311 (2006) 185–192.
[41] D. Wang, A. Villa, F. Porta, D. Su, L. Prati, Chem. Commun. (2006) 1956–1958.
[42] D.I. Enache, D.W. Knight, G.J. Hutchings, Catal. Lett. 103 (2005) 43–52.
[43] G. Li, D.I. Enache, J.K. Edwards, A.F. Carley, D.W. Knight, G.J. Hutchings, Catal. Lett. 110 (2006) 7–13.
[44] D.I. Enache, J.K. Edwards, P. Landon, B. Solsona-Espriu, A.F. Carley, A.A. Herzing, M. Watanabe, C.J. Kiely, J.D.W. Knight, G.J. Hutchings, Science 311 (2006) 362–365.
[45] G.J. Hutchings, S. Carrettin, P. Landon, J.K. Edwards, D. Enache, D.W. Knight, Y.-J. Xu, A.F. Carley, Top. Catal. 38 (2006) 223–230.
[46] V.R. Choudhary, R. Jha, P. Jana, Green Chem. 9 (2007) 267–272.
[47] H. Tsunoyama, H. Sakurai, T. Tsukuda, Chem. Phys. Lett. 429 (2006) 528–532.
[48] A. Abad, C. Almela, A. Corma, H. Garcia, Chem. Commun. (2006) 3178–3180.
[49] A. Abad, C. Almela, A. Corma, H. Garcia, Tetrahedron 62 (2006) 6666–6672.
[50] P.G.N. Mertens, M. Bulut, L.E.M. Gevers, I.F.J. Vankelecom, P.A. Jacobs, D.E. De Vos, Catal. Lett. 102 (2005) 57–61.
[51] P.G.N. Mertens, I.F.J. Vankelecom, P.A. Jacobs, D.E. De Vos, Gold Bull. 38 (2005) 157–162.
[52] J. Guo, H. Lou, H. Zhao, D. Chai, X. Zheng, Appl. Catal. A 273 (2004) 75–82.
[53] J. Guo, H. Lou, H. Zhao, X. Wang, X. Zheng, Mater. Lett. 58 (2004) 1920–1923.
[54] T. Hayakawa, S. Suzuki, J. Nakamura, T. Uchijima, S. Hamakawa, K. Suzuki, T. Shishido, K. Takehira, Appl. Catal. A 183 (1999) 273–285.
[55] J.P. Wilcoxon, R.L. Williamson, R. Baughman, J. Phys. Chem. 98 (1993) 9933–9950.
[56] A. Slistan-Grijalva, R. Herrera-Urbina, J.F. Rivas-Silva, M. Avalos-Borja, F.F. Castillon-Barraza, A. Posada-Amarillas, Physica E 27 (2005) 104–112.
[57] P.G.N. Mertens, H. Poelman, X. Ye, I.F.J. Vankelecom, P.A. Jacobs, D.E. De Vos, Catal. Today 122 (2007) 352–360.
[58] J. Hu, L. Chen, K. Zhu, A. Suchopar, R. Richards, Catal. Today 122 (2007) 277–283.
[59] N. Dimitratos, J.A. Lopez-Sanchez, D. Morgan, A. Carley, L. Prati, G.J. Hutchings, Catal. Today 122 (2007) 317–324.
[60] D.I. Enache, D. Barker, J.K. Edwards, S.H. Taylor, D.W. Knight, A.F. Carley, G.J. Hutchings, Catal. Today 122 (2007) 407–411.

[61] H. Tsunoyama, H. Sakurai, Y. Negishi, T. Tsukuda, J. Am. Chem. Soc. 127 (2005) 8374–9375.
[62] B. Pawelec, A.M. Venezia, V. La Parola, E. Cano-Serrano, J.M. Campos-Martin, J.L.G. Fierro, Appl. Surf. Sci. 242 (2005) 380–391.
[63] A.M. Venezia, L.F. Liotta, G. Pantaleo, V. La Parola, G. Deganello, A. Beck, Zs. Koppany, V. Frey, D. Horvath, L. Guczi, Appl. Catal. A 251 (2003) 359–368.
[64] H. Liu, G. Mao, S. Meng, J. Mol. Catal. 74 (1992) 275–284.
[65] A. Villa, C. Campione, L. Prati, Catal. Lett. 115 (2007) 133–136.
[66] P.G.N. Mertens, F. Cuypers, P. Vandezande, X. Ye, F. Verpoort, I.F.J. Vankelecom, D.E. De Vos, Appl. Catal. A 325 (2007) 130–139.
[67] C. Baatz, N. Thielecke, U. Prüβe, Appl. Catal. B 70 (2007) 653–660.
[68] D. Yin, L. Qin, J. Liu, C. Li, Y. Jin, J. Mol. Catal. A 240 (2005) 40–48.
[69] J.H. Zhong, Y.Q. Yang, J.M. Shen, J.A. Wang, J. Mol. Catal. A 237 (2005) 182–190.
[70] G. Mul, A. Zwijnenburg, B. van der Linden, M. Makkee, J. Catal. 201 (2001) 128–137.
[71] P.K. Iler, The Chemistry of Silica, Wiley, New York, 1979.
[72] M. Pattanaik, S.K. Bhaumik, Mater. Lett. 44 (2000) 252–360.
[73] C. Binet, M. Daturi, J.-C. Lavalley, Catal. Today 50 (1999) 207–225.
[74] P.F. Rossi, G. Busca, V. Lorenzelli, M. Lion, J.-C. Lavalley, J. Catal. 109 (1998) 378–386.
[75] P. Haider, A. Baiker, J. Catal. 248 (2007) 175–187.
[76] W.-C. Li, M. Comotti, A.-H. Lu, F. Schuth, Chem. Commun. (2006) 1772–1774.
[77] J.-D. Grunwaldt, H. Teunissen, US 6692713, Topsoe Haldor (2004).
[78] F.M.P.R. van Laar, D.E. De Vos, F. Pierard, A. Kirsch-De Mesmaeker, L. Fiermans, P.A. Jacobs, J. Catal. 197 (2001) 139–150.
[79] J. Wahlen, D.E. De Vos, P.A. Jacobs, V. Nardello, J.-M. Aubry, P.L. Alsters, J. Catal. 249 (2007) 15–23.
[80] P.G.N. Mertens, J. Wahlen, X. Ye, H. Poelman, D.E. De Vos, Catal. Lett. 118 (2007) 15–21.